A vision of versatile bottom-up construction of diverse macromolecules on a surface.

Journal:	*ACS Nano*
Manuscript ID:	nn-2013-03016m
Manuscript Type:	Article
Date Submitted by the Author:	14-Jun-2013
Complete List of Authors:	Haq, Sam; The University of liverpool, Surface Science Research Centre and Department of Chemistry Hanke, Felix; Accelrys Ltd, Persson, Mats; The University of Liverpool , Surface Science Research Centre and Department of Chemistry Amabilino, David; Institut de Ciència de Materials de Barcelona (CSIC), Laboratori de Materials Orgànics Raval, Rasmita; The University of liverpool, Surface Science Research Centre and Department of Chemistry

A vision of versatile bottom-up construction of diverse macromolecules on a surface

Sam Haq,[¶] Felix Hanke,[⊥¶] Mats Persson,[¶] David B. Amabilino[§] and Rasmita Raval[¶]**

[¶] Surface Science Research Centre, Department of Chemistry, University of Liverpool, L69 3BX, Liverpool, U.K. E-mail: Raval@liv.ac.uk

[⊥] Current address: Accelrys, Ltd., 334 Science Park, Cambridge, CB4 0WN

[§] Institut de Ciència de Materials de Barcelona (ICMAB-CSIC), Campus Universitari, 08193-Bellaterra, Catalonia, Spain. E-mail: amabilino@icmab.es

KEYWORDS : aromatic hydrocarbons - nanomaterials -on-surface synthesis-porphyrins- surface chemistry –C-H bond activation

ABSTRACT : The hetero-coupling of organic building blocks to give complex multicomponent macromolecules directly at a surface holds the key to creating advanced molecular devices. While 'on-surface' synthesis with pre-functionalized molecules has recently led to specific one- and two- component products, a central challenge is to discover universal connection strategies that are applicable to a wide range of molecules. Here, we show that direct activation of C-H bonds intrinsic to π–functional molecules unleashes a highly generic route for connecting different building blocks on a copper surface. Scanning tunneling microscopy (STM) reveals that covalent π-functional macromolecular heterostructures, displaying diverse compositions structures and topologies, are created with ease from seven distinct building blocks (including porphyrins, pentacene and perylene). By exploiting differences in C-H bond reactivity we also demonstrate controlled synthesis of specific products, such as block copolymers. Our 'pick-mix-and-link' strategy opens up the capability to generate libraries of multivariate macromolecules directly at a surface that, in conjunction with nanoscale probing techniques, could accelerate the discovery of functional interfaces and molecular materials.

The formation of a broad mix of multicomponent macromolecules- comprising combinations of operative units derived from simple molecular building-blocks- is a key step in generating complexity, diversity and advanced functionality in synthetic materials. Pertinently, compositional and topological diversity of macromolecules are the hallmarks of evolved systems biology and emergent systems chemistry and are fundamental for realizing complex functions.[1] Introducing such macromolecular complexity *at a surface* is a major research challenge for achieving new and improved functions in molecular electronics, biomedical devices, sensors, energy harnessing and catalysis.[2,3,4] The covalent hetero-coupling of organic building blocks directly on a surface to give complex multicomponent macromolecules holds the key to creating such advanced systems. Recently, 'on-surface' synthesis with pre-functionalized molecules has led to specific one- and two-component products with remarkable efficiency[5-19]. However, while certain reactions are known to proceed smoothly on surfaces[20,21], a central challenge in the field is to discover universal yet specific connection strategies that are applicable to a wide range of molecules. This is particularly important since a fundamental barrier to bottom-up 'on-surface' synthesis of molecular devices is that the macromolecular architectures required to deliver advanced functions are largely unknown. This situation can make it restrictive to use the purely logical protocols of synthetic chemistry, which are confined towards specific macromolecule outputs. It may, therefore, be timely to switch to scenarios reminiscent of synthetic biology and systems chemistry[1] where many different molecules are connected via highly parallel syntheses to give diverse and complex macromolecules, which can eventually be assayed for function in an analogous way to combinatorial strategies toward drug and materials discovery.[22,23]

Multivariate heterostructures could, in principle, be generated at surfaces using specifically pre-functionalized molecules, however, this can require significant synthetic effort to create the requisite molecular building blocks. We, therefore, have pursued an alternative route by exploiting surface reactivity to directly activate C-H bonds that are ubiquitous in organic building blocks. Thus, we have previously linked porphyrins together at the Cu(110) surface via C-H scission followed by either direct C-C[24] or C-metal-C bond[25,26] formation. During these processes, metalation of the porphyrin can also occur, in itself an interesting process.[27,28] Here, the wider generality of this approach is established and we show that the direct activation of C-H bonds intrinsic to organic molecules unleashes a highly generic route for connecting different building blocks on a copper surface. Specifically, we demonstrate that the C-H group can be a highly effective synthon and provides routes that enable many different types of organic components to be linked together at a surface (Figure 1). Scanning tunneling microscopy (STM) reveals that covalent π-functional macromolecular heterostructures, displaying diverse compositions, structures and topologies, are created with ease from seven building blocks. By exploiting differences in C-H bond reactivity we also demonstrate controlled synthesis of specific products. Our 'pick-mix-and-link' strategy opens up the capability to generate libraries of multivariate macromolecules at surfaces. We note that the availability of surface nanoscale probing techniques would enable individual interrogation of each structure and, thus, could accelerate the discovery of functional interfaces and molecular materials. The development of this new surface chemistry also has direct parallels in the related contemporary challenges C-H bond activation[29] and carbon metathesis[30] for chemical synthesis.

The functional units used here - namely pentacene, perylene, and different porphyrins (Figure 1) - are successfully employed in molecular electronics[31]. Whereas the former two possess sp^2

hybridized carbon atoms only, the latter have porphyrinyl, phenyl or methyl moieties, with sp^2 and sp^3 hybridized carbon atoms. The components have different sizes, symmetries and geometries, allowing easy identification by scanning tunneling microscopy (STM) so that the molecular constitution of each covalently linked heterostructure can be mapped together with the regioselectivity of the reaction that produces it. We show that each component can react in a number of different ways, and combinations of components lead to the highly varied topologies and heterostructures shown in Figure 1. Some of these structures are familiar from polymer syntheses – such as the branched ladder, the block polymer (including the 'guitar fret') or the rod-coil – but other combinations such as the 'capped ladder' and the 'key' are quite unique outputs of selective surface chemistry, and represent new classes of macromolecular entities that have no counterpart in homogeneous organic synthesis.

RESULTS AND DISCUSSION

1D Oriented Random and Block Co-Polymers: First, the creation of unidirectional heterostructures on Cu(110) using 2H-porphyrin (**1**) and Zn(II)-diphenylporphyrin (**2**) was investigated. We have established previously, via detailed STM and periodic DFT calculations, that that each component alone can generate 1D organocopper homopolymers[25] via edge-to-edge porphyrin–Cu-porphyrin connections where cleavage of the sp^2 C-H bond occurs at the 3, 5 and 7 positions and leads to formation of one, two or three C-Cu-C bonds. Both oligoporphyrins grow preferentially along the [001] surface direction, as a result of the geometry-match of the macromolecule with the underlying surface.[26]

Here, we endeavored to create a co-oligomer by co-adsorbing porphyrins **1** and **2** on the Cu(110) surface at room temperature and then heating to 650 K. STM images, Figure 2a, show that the two components indeed link together to form unidirectional linear co-oligomers. Each component within an oligomer can be identified, with **1** producing square images with straight edges, while **2** displays the phenyl groups, giving a serrated appearance along the polymer length. The porphyrins are distributed randomly, generating a wide variety of heterostructures, from totally random oligomers, Figure 2a(i, ii), to block oligomers in which a section derived from one porphyrin is followed by a section composed of the other. High resolution STM images, Figure 2a(iii), confirm that the organometallic linkage is also employed in the co-polymer, with the connecting metal atoms clearly imaged, and the individual units separated by the expected distance of 10.8 Å[25] (Figures 2, 3).

The defined orientation and connectivity of the copolymers shown in Figure 2 is in keeping with the detailed data we have already obtained on the 1D homopolymer of **1** that is formed on this surface.[25,26,32] Figure 3 summarizes the structure of the oriented polymer of **1,** its registry and preferential orientation with the underlying surface, and the C-Cu-C organometallic connections that drive this assembly, as deduced from experimental STM, periodic DFT and simulated STM[25, 26] data. It is clear that this organometallic covalent chemistry is also carried over to the co-polymer systems shown in Figure 2. Specifically, the directionally selective growth of this copolymer is a result of the identical molecular cores, which are subject to the commensurability match with the underlying surface[26], but which also enable more inert functionalities to be located in the available lateral positions of the macrocycle, thus allowing compositional variation.

From Prolific to Controlled Outputs: The 'mix-and-heat' experiment above generates an enormous diversity of structures. However, the output can be controlled by exploiting the fact that Zn(II)-diphenylporphyrin **2** reacts at a much lower temperature of 560K compared to 650K for porphyrin **1**. Thus, the sequence of connectivity can be tailored to predispose the system towards block copolymer creation. Hence, porphyrin **1** was first adsorbed at the surface and heated to 650K to link the like components together. This was followed by adsorption of **2** and heating to the lower temperature of 560K, where only **2**-**2** or **2**-**1** porphyrin connections can be made, while **1**-**1** are inaccessible. This altered synthesis protocol produces a different distribution of heterostructures, Figure 2b, in which 'guitar fret' block copolymers, Figure 2b(ii), and capped structures, Figure 2b(iii and iv) are favored. Thus, the inherent difference in C-H bond reactivity for the two different molecules opens up a route to selective heterostructure growth without recourse to synthesizing specifically functionalized precursors.

Connecting Dissimilar Molecules- Arenes plus Porphyrins: Next, we investigated whether C-H activated coupling could be extended to π-functional hydrocarbons by depositing pentacene (**3**) onto Cu(110) and heating to 600K. STM images show the formation of discrete dimer sandwich structures, with two molecules joined lengthwise and parallel with each other by interlinking Cu atoms between them, Figure 4a(i). The bright spots imaged in between indicate C-Cu-C connections along the [001] surface direction, with up to five Cu atoms incorporated to create the dimer sandwich, Figure 4a(ii). Density Functional calculations for the copper-bridged pentacene dimer in the gas phase show that the addition of each Cu atom to create the organometallic C-Cu-C linkage corresponds to a gain of about 0.5-0.6 eV. Thus, the 5-Cu bonded dimer yields an energy gain of about 3eV associated with the breaking of all five C-H bonds along the length of each pentacene molecule and formation of five C-Cu-C linkages,

generating the structure in Figure 4a(iii). Furthermore, the five connecting Cu atoms, held 2.44 Å apart, closely match the Cu-Cu distance (2.5 Å) in the [110] surface direction, enabling their easy accommodation on the surface as a local 'added row' structure.[26] This situation would orientate the pentacene long-axis parallel to the Cu(110) rows, which agrees with STM observation (Figure 4a.). This orientation and surface registry is also maintained if the number of connecting atoms along the length is reduced, e.g. the three-Cu configuration, shown in Figure 4a(iii).

The 3-pentacene sandwich, Fig 4a(iii), was also calculated in order to gauge the creation of trimer and higher-order pentacene structures stacked along the [001] direction. For the trimer sandwich, we also find a very similar energy for forming each C-Cu-C linkage as for the pentacene dimer, but the computed Cu-Cu distance between the two connecting rows across the molecule is 6.72 Å, which is ~93% of a double inter-row spacing in the [001] direction (7.26 Å). These 3-pentacene systems are, therefore, expected to be more strained on the surface, explaining the preference for creating dimer pentacene sandwiches at low coverages. We note, however, at higher coverages, formation of trimer and higher order pentacene units is experimentally observed, presumably because the energy gain that accompanies the formation of C-Cu bonds compensates for the surface mismatch.

Coupling of two very different molecules is demonstrated when 2H-porphyrin **1** and pentacene were co-adsorbed and reacted together by heating to 650K under low coverage (<0.25 monolayer) conditions. Interestingly, modular construction behavior was observed in which dimer and monomer pentacene bind to the 1D porphyrin organometallic wires, Figure 4b. Inter-module connections were observed at two positions, either at the side of the oligoporphyrin long edge to produce simple and complex key topologies, Figure 4b(i, ii), or at the porphyrin chain ends to give capped ladder topologies, Figure 4b(iii). In both cases, bright regions were imaged

at the inter-module boundaries, indicative of copper atoms linking the two covalent modules together, Figure 4b(i-iii). We also note that when the pentacene caps the porphyrin oligomers, it acts as a terminating group, with further connections to additional porphyrin units disfavored. Therefore, pentacene acts to limit local heterostructure growth on this copper surface.

At high coverages, complex networks form in which pentacene trimers, dimers and monomers are coupled with porphyrin monomers and oligomers via Cu atoms, enabling connectivity along many different directions as shown in the STM image in Figure 5. High resolution STM images, in which the inter-connecting Cu atoms are imaged brighter than the pentacene molecules, show the preponderance and variety of organometallic C-Cu-Cu connections that are facilitated. The presence of multi-pentacene sandwiches is clearly observed under such conditions, which show the brighter connecting Cu atoms, the dimmer pentacene molecules at the outer edges of the sandwich, with the inner pentacenes imaging darker, Fig 5b .

Creating Further Complex Bi-Component Topologies: We further extended our repertoire of connections by: (i) combining systems that couple via C-Cu-C organometallic couplings with those that connect through C-C coupling; and (ii) by connecting different topologies (rods, branched networks, coils) together. Porphyrin **1** is an excellent rod-former (Figure 2) and our aim was to link these C-Cu-C coupled rods to branches and coils created via C-C coupling. Branched connectivity is provided by tetramesitylporphyrin (**4**) where we have previously shown[24] that surface activation of the methyl group at the *para* position of the benzene, generates a $CH_2^{\bullet}$ radical group which homocouples the porphyrins via C-C covalent links. Thus, four C-C connections can potentially be forged by **4**, at each mesityl group, leading to branched covalent

nanostructures, Fig 6a, 7d. A very different topology is created when perylene (**5**) is coupled on the surface, forming a random coil structure with no clearly identifiable repeating residue, Figure 6c(i), 7a, in a similar way to a recently described dehydrogenation of heteroaromatics.[33] This topology is also displayed by covalent self-coupling of rubrene and coronene at this surface, where multiple connections lead to attractive branched and coiled structures, Figure 7b,c. This behavior is attributed to C-C linkages, which are randomly positioned with respect to the surface, that is, the macromolecular architecture is not prescribed by the surface, in contrast to all the other examples shown above.

When porphyrins **1** and **4** are reacted by co-deposition at room temperature and heating to 605K, a series of complex bi-component branched motifs are created, linking via the methyl groups of **4** and the corners of **1**. When a building block of **4** reacts with four units of **1**, a four-connected clover leaf structure is generated, as seen in Figure 6a(ii). This clover leaf adduct combines further with individual units of **1** or **4** to propagate both regular and irregular two-component branched nanostructures (Figure 6a(i, iii)). Alternatively, a more modular construction is enacted whereby porphyrin **1** is first reacted to give 1D organometallic rods, and then **4** adsorbed and reacted to give branched structures in which both **4** and residual **1** units combine. The rod and branched topologies further link together to give windmills (W), trees (T) and double propellers (DP), as seen in Figure 6b(i, ii) and branched-ladder (BL) macromolecules as in Figure 6b(i), where chains of **1** grow away from different methyl groups of **4**, indicating that **4** is a suitable linker for the rod structures.

Adsorption and surface oligomerization of 2H-porphyrin (**1**), followed by addition and heating of perylene (**5**) to 620K results in block copolymers with an apparent rigid rod-coil structure, Figure

6c(i-iii). The 1D order in the porphyrin segment is maintained, from which random chains of the perylene oligomer grow away in all directions of the surface.

Three Component Heterostructures: The C-H synthon is ubiquitous and its surface activation to drive C-H bond breaking and create C-C and C-M-C couplings provides the opportunity to connect many different molecular building blocks together. We demonstrate this capability by generating three-component heterostructures that exploit the different connectivity preferences of the molecular components used up to this point. The reaction of porphyrins **1** and **2** was first coupled sequentially to give 1-D block copolymer chains, and subsequent reaction of pentacene **3** leads to its attachment at the end or the side of the chain, to give capped and key structures, and more complex inter-chain connections (Figure 8a). The detail of a 3-component key is shown in Figure 8b, with pentacene attached to the side of porphyrin **1** components in the mixed chain and capping porphyrin **2** at the chain end. Although there can exist independent pentacene dimers present on the surface (as a result of homocoupling in the spaces between the porphyrin rows) they are the minority structure. This observation demonstrates that, in this kind of complex multicomponent system, the local stoichiometry of the combining molecules will influence the outcome of the coupling on the surface. Thus, diffusion[34,35.] between growing chains will lead to very different local concentrations and, therefore, different macromolecular compositions. This shows the beginning of complex connectivity selection by the pentacene component, and the generation of a diversity of three component macromolecular structures that are at present inaccessible by any other solution or surface-based bottom-up protocol. Furthermore, this provides proof-of-principle that, theoretically, *there is no upper limit* to how many different components can be coupled at a surface using our generic method.

CONCLUSION

The coupling of different organic building-blocks by a general surface-mediated intramolecular C-H bond-breaking and intermolecular bond-making mechanism has been demonstrated on a copper surface. Thus, a range of macromolecules is formed in parallel and selective ways, creating complexity and diversity from simple components. Coupling via the C-H synthon provides a highly universal and inexpensive approach to covalently link together many different organic entities at surfaces. Thus, we demonstrate an easy 'pick-mix-and-link' approach that enables the following strengths to be combined:

'**Easy Pick'**: To extend coupling to a wide-range of molecules, we have utilized a fundamentally different approach, which *does not* require pre-functionalisation of the molecular building block. Instead, we use the C-H bond as a generic synthon, which is ubiquitous in all organics and enables a wide range of cheap and accessible building-blocks to be picked for synthesis. We have successfully used this approach for seven different organic components that are all employed in molecular electronics, and anticipate the breadth of this approach to encompass a huge range of molecular building blocks.

'**Easy Mix'**: Activation of C-H bonds is a contemporary challenge across chemistry. Here, we harness surface reactivity to activate many types of C-H bonds (porphyrinyl, arene, alkyl) so that readily available molecules are made amenable for mixing. Our method generates complex organic heterostructures with ease. This provides proof-of-principle that, theoretically, there is no upper limit to how many different components can be coupled at a surface using our generic method, thus vastly increasing on-surface linking capability and the chance to generate vast macromolecular libraries of combinations of functional components with different connectivities by varying deposition and annealing orders.

'**Easy Link'**: Since the molecular targets for successful devices are limited, it would be highly advantageous to unleash parallel syntheses of many different outputs. Here, we exploit the bond-making capability of a surface to create many different C-C and C-metal-C covalent linkages, leading to facile generation of diverse and complex macromolecular libraries directly on the surface. The range of structures we have created are unparalleled in the field as summarized in Fig 9. Specifically, we have linked many different topologies together (rods, bricks, branches, coils) to create complex architectures. Some of these structures are familiar from polymer syntheses – e.g. branched ladder, the block polymer (guitar fret) or the rod-coil – but other combinations such as the 'capped ladder', the 'key' and the 'double propeller' are unique outputs of surface chemistry, and represent *new classes of macromolecular entities that have no counterpart in organic synthesis*. The fecundity and multiple-output capability of our approach demonstrates that surface systems can emulate synthetic biology approaches and rapid discovery methods in which highly parallel synthesis occurs, leading to diverse pools of complex macromolecules, from which selection of the fittest can be made. This is particular important since the organic macromolecules and architectures required for successful molecular devices are largely unknown. Further, we show that it is possible to move beyond prolific outputs and achieve control of on-surface macromolecular synthesis when required, by exploiting the specific C-H reactivity encoded in each building block. For example, we tailor the surface reaction so macromolecules are predisposed toward block copolymers rather than random ones.

'Clean Link': Finally, in our systems, the cleavage of the C-H bond only generates H_2 via recombinative desorption, i.e. we achieve the linkage of organic components *without* depositing contamination on the surface (as can happen when using pre-functionalised molecules, leading to

surface contamination) - this is a significant achievement for device construction, because only the π-functional products are adhered to the surface at the end of the process.

This work evokes modular approaches recently demonstrated for assembling new classes of porous covalent organic molecular cages[36], complexed polymers[37] and multivariate libraries of metal-organic materials[38], where new complex arrangements of functional groups are generated leading to unexpected properties. Similarly, we anticipate that our 'pick-and-mix-and-link' approach at a surface will pave the way for *in situ* screening of different individual covalent structures for specific functions such as nanomagnetism, conductance, sensing, reactivity, energy-transfer, and other molecular device types, using local probe techniques[22,39]. Once desired macromolecular structures are identified, our approach is also viable for programming specific products by exploiting the unique C-H bond reactivity encoded in each component and its fit with the surface, which can be finessed to suit via tailoring of both the molecule and the substrate.

Methods

(i) Experimental Details: STM experiments were performed under ultra-high vacuum (UHV) conditions using a Specs STM 150 Aarhus instrument. The STM was calibrated to better than 5% accuracy by measuring the atomic distances of the clean Cu(110) surface. All measurements were taken in constant current mode, using a tungsten tip and at a base pressure of 1.5×10^{-10} mbar. Bias voltages are measured at the sample ($V = V_{sample}$). STM images were enhanced for brightness and contrast using the Image SxM programme[40]. The Cu(110) surface was prepared in a UHV chamber using Argon ion sputtering and annealing cycles, and atomic flatness and cleanliness were checked by STM prior to dosing the molecule. H_2-porphyrin (**1**), and Tetra(mesityl)porphyrin (**4**) (Frontier Scientific) and pentacene (**3**), perylene (**5**) (Sigma Aldrich, all >98% purity) were used as purchased and sublimed onto the Cu(110) surface, which was held at room temperature during deposition. 5,15-Diphenylporphyrin was purchased from Frontier Scientific, and the zinc(II) complex was synthesized as described below.

ii) **Synthesis:** The zinc(II) complex was synthesized by reaction with Zinc(II)acetate in dimethylformamide at 120 ºC for 3 hours. The mixture was cooled and water was added. The precipitate was filtered, washed with water and diethyl ether and air dried. The resulting material was chromatographed by flash column chromatography on silica using dichloromethane-hexane 4-6 as eluent. The product was further purified by crystallization from toluene. The product gave the characteristic spectroscopic data for this Zn(II)porphyrin[41] with no indication of the free base porphyrin in the UV-visible spectrum, laser desorption-ionization mass spectrum or in the 1H NMR spectrum.

iii) **Computational Details**: The organometallic porphyrin chains of 1 on Cu(110)[25,26] were modeled via density functional calculations using the VASP code[42]. Plane waves were used as a basis set with an energy cut-off of 400 eV. Valence electron-core interactions were included using the projector augmented wave method[43] and the generalized gradient approximation (PW91) was used for the exchange-correlation functional[44]. The calculations of the periodic chain structures were carried out in a 3x6 surface unit cell using a 4x3x1 k-point grid. The copper surface was modeled using a four layer slab, where the bottom two layers were fixed in their calculated bulk positions and the top two layers were allowed to relax. The vacuum separation between the copper slabs was 16.8 Å, leaving about 15 Å between the molecule and the back of the next slab. Adsorption and coupling geometries were calculated by placing a porphyrin molecule above the surface and allowing all molecular atoms and the top two layers of the copper slab to relax until all the forces on the atoms were less than 0.01 eV/Å. STM images were calculated in the Tersoff-Hamann approximation[45] using the implementation by Lorente and Persson[46].

To study the adsorption process, calculations were performed for the full adsorbate-surface system, and also on the isolated molecular overlayer, the isolated Cu-porphyrin chains, the isolated radicals (e.g. chains without the Cu atoms) and the isolated copper substrate in the same calculation supercell. The adsorption energies were computed using:

$$E_{ads} = E_{sys} - E_{subs} - E_{Cu\text{-}P,vac} - n_{Cu}E_{Cu,ads} + 2n_{Cu}E_{H,ads}, \quad (1)$$

where E_{sys} is the energy of the system, E_{subs} and $E_{Cu^-P,vac}$ are the energies of the metal substrate and the Cu-porphyrin in vacuum, $E_{Cu,ads}$ and $E_{H,ads}$ are the adsorption energies of single adsorbed Cu and H-atoms respectively, and n_{Cu} is the number of Cu adatoms (C-Cu-C couplings) per porphyrin molecule in the system. The bonding electron density in Figure 3 of manuscript was visualized by obtaining the total density for the adsorbed Cu-porphyrin complex and subtracting the total electron density of the Cu slab (with the adatoms) and the radical.

All DFT calculations of pentacene-pentacene coupling were performed using the PBE density functional[47] as implemented in the all electron numeric atomic orbital computational package FHI-aims[47]. All structures have been optimized using the FHI-aims tight basis set (atomic basis functions H: minimal basis + sp spd s, C: minimal basis + spd spdfg, Cu: minimal basis + spdfg), and until the maximal force on each atom was less than 0.01 eV/Å.. The bonding energy of the pentacene dimers and trimers were obtained in similar way as in Eq.(1) but now with $E_{subs}=E_{Cu^-P,vac}=0$, $E_{Cu,ads}$ being the energy of a Cu atom in vacuum and $E_{H,ads}$ being the binding energy of the H_2

molecule. Note that the dissociative adsorption of a hydrogen molecule on a copper surface is nearly thermoneutral [ref].The binding energies for the pentacene dimer with three and five C-Cu-C linkages were -1.49 and -3.06 eV, respectively and -5.94 eV for the pentacene with 10 C-Cu-C linkages. A detailed comparison to previous work on porphyrins[25,26] confirmed that the energetic hierarchies obtained for C-Cu-C linkages in vacuum are very similar to those obtained on surfaces but at a small fraction of the computational cost. In addition we calculated the interatomic distance of all possible substitutions of two Cu adatoms attaché to a pentacene. From these calculations, we identified two possible coupling configurations that are commensurate with the surface: adatoms replacing neighbouring H-atoms on the "sides" of the pentacene and adatoms replacing H-atoms straight across the pentacene backbone.

AUTHOR INFORMATION

Corresponding Author

* Address correspondence to amabilino@icmab.es or raval@liv.ac.uk

Conflict of Interest: The authors declare no competing financial interest.

ACKNOWLEDGMENT

The research was supported by: the UK EPSRC grant EP/F00981X/1 and EU ITN project SMALL (grant agreement 238804) for R.R.; the MINECO (Spain), under the project CTQ2010-16339 and the Generalitat de Catalunya (Project 2009 SGR 158) for D.B.A.; the EU project ARTIST (grant agreement no. 243421) for FH and MP and the Swedish Research Council (VR) for MP.

REFERENCES

1. Ludlow, R.F.; Otto, S. Systems Chemistry. *Chem. Soc. Rev.* **2008**, *37*, 101-108.
2. Smits, E.C.P.; Smits, E.C.P. ; Mathijssen, S.G.J.; van Hal, P.A.; Setayesh, S.; Geuns, T.C.T.; Mutsaers, K.A.H.A.; ECantatore, E.; Wondergem, H.J.; Werzer, O.; Resel, R. Kemerink, M.; Kirchmeyer, S.; Muzafarov, A.M.; Ponomarenko, S.A.; de Boer, B.; Blom, P.W.M; de Leeuw, D.M. Bottom-up organic integrated circuits. *Nature* **2008**, *455*, 956-959.
3. Aida, T.; Meijer, E.W.; Stupp, S.I. Functional Supramolecular Polymers *Science* **2012**, *335*, 813-817.
4. Koepf, M.; Cherioux, F.; Wytko, J.A.; Weiss, J. 1D and 3D surface-assisted self-organization. Coord. Chem. Rev. 2012, 256, 2872-2892
5. Grill, L.; Dyer, M.; Lafferentz, L.; Persson, M.; Peters, M.V.; Hecht, S. Nano-architectures by covalent assembly of molecular building blocks. *Nature Nanotech.* **2007**, *2*, 687-691.
6. Weigelt, S.; Busse, C.; Bombis, C.; Knudsen, M.M.; Gothelf, K.V.; Lægsgaard, E.; Besenbacher, F.; Linderoth, T.R. Covalent interlinking of an aldehyde and an amine on a Au(111) surface in ultrahigh vacuum. *Angew. Chem. Int. Ed.* **2008**, *47*, 4406-4410.
7. Treier, M.; Fasel, R.; Champness, N.R.; Argent, S.; Richardson, N.V. Molecular imaging of polyimide formation. *Phys. Chem. Chem. Phys.* **2009**, *11*, 1209-1214.

8. Jensen, S.; Fruchtl, H.; Baddeley, C.J. Coupling of Triamines with Diisocyanates on Au(111) Leads to the Formation of Polyurea Networks. J. Am. Chem. Soc.2009, 131, 16706-16713.

9. Elemans, J.A.A.W.; Lei, S.B.; De Feyter, S. Molecular and Supramolecular Networks on Surfaces: From Two-Dimensional Crystal Engineering to Reactivity. *Angew. Chem. Int. Ed.* **2009**, *48*, 7298-7332.

10. Cai, J.; Ruffieux, P.; Jaafar, R.; Bieri, M.; Braun,T; Blankenburg, S.; Matthias, M.; Seitsonen, A.P.; Saleh, M.; Feng, X.; Mullen, K.; Fasel, R. Atomically precise bottom-up fabrication of graphene Nanoribbons. *Nature* **2010**, *466*, 470-473.

11. Matena, M.; Stöhr, M.; Riehm, T.; Björk, J.; Martens, S.; Dyer, M. S.; Persson, M.; Lobo-Checa, J.; Müller, K.; Enache, M.; Wadepohl, H.; Zegenhagen, J.; Jung, T. A.; Gade, L. H. *Chem. Eur. J.* **2010**, *16*, 2079-2091.

12. Bartels, L. Tailoring molecular layers at metal surfaces. *Nature Chem.* **2010**, *2*, 87-95.

13. Lipton-Duffin, J.A.; Miwa, J.A.; Kondratenko, M.; Cicoira, F.; Sumpter, B.G.; Meunier, V.; Perepichka, D.F.; Rosei, F. Step-by-step growth of epitaxially aligned polythiophene by surface-confined reaction. *Proc. Natl. Acad. Sci. USA* **2010**, *107*, 11200-11204.

14. Abel, M.; Clair, S.; Ourdjini, O.; Mossoyan, M.; Porte, L. Single Layer of Polymeric Fe-Phthalocyanine: An Organometallic Sheet on Metal and Thin Insulating Film. *J. Am. Chem. Soc.* **2011**,*133*, 1203-1205.

15. Lackinger, M.; Heckl, W. M. A STM perspective on covalent intermolecular coupling reactions on surfaces. *J. Phys. D-Appl. Phys.* **2011**, *44*, Article Number: 464011.

16. Lafferentz, L.; Eberhardt, V.; Dri, C.; Africh, C.; Comelli, G.; Esch, F.; Hecht, S.; Grill, L. Controlling on-surface polymerization by hierarchical and substrate-directed growth. *Nature Chemistry* **2012**, *4*, 215-220.

17. Tanoue, R.; Higuchi, R.; Ikebe, K.; Uemura, S.; Kimizuka, N.; Stieg, A.Z.; Gimzewski, J.K.; Kunitake, M. In Situ STM Investigation of Aromatic Poly(azomethine) Arrays Constructed by "On-Site" Equilibrium Polymerization. *Langmuir* **2012**, *28*, 13844-13851.

18. Greenwood, J.; Fruechtl, H.A.; Baddeley, C.J. Surface-Confined Reaction of Aliphatic Diamines with Aromatic Diisocyanates on Au{111} Leads to Ordered Oligomer Assemblies. J. Phys. Chem C **2013**, *117*, 4515-4520.

19. Greenwood, J.; Baddeley, C. J. Formation of Imine Oligomers on Au under Ambient Conditions Investigated by Scanning Tunneling Microscopy. *Langmuir* **2013**, *29*, 653-657

20. Treier, M.; Pignedoli, C.A.; Laino, T.; Rieger, R.; Mullen, K.; Passerone, D.; Fasel, R. Surface-assisted cyclodehydrogenation provides a synthetic route towards easily processable and chemically tailored nanographenes. *Nature Chem.* **2011**, *3*, 61-67.

21. Dinca, L.E.; Fu, C.Y.; MacLeod, J.M.; Lipton-Duffin, J.; Brusso, J.L.; Szakacs, C.E.; Ma, D.L.; Perepichka, D.F.; Rosei, F. Unprecedented Transformation of Tetrathienoanthracene into Pentacene on Ni(111). *ACS Nano* **2013**, *7*, 1652-1657

22. DiLullo A. Chang, S.H.; Baadji, N.; Clark, K.; Klockner, J.P.; Prosenc, M.H.; Sanvito, S.; Wiesendanger, R.; Hoffmann, G.; Hla, S.W. Molecular Kondo Chain. *Nano Letters* **2012**, *12*, 3174.

23. Xiang, D.; Sun X.; Briceño, G.; Lou, Y.; Wang, K.A.; Chang, H.; Wallace-Freedman, W.G.; Chen, S.W.; Schultz, P.G. A combinatorial approach to materials discovery. *Science* **1995**, *268*, 1738-1740.

24. In't Veld, M.; Iavicoli, P.; Haq, S.; Amabilino, D.B.; Raval, R. Unique intermolecular reaction of simple porphyrins at a metal surface gives covalent nanostructures. *Chem. Commun*. **2008**, 1536-1538.

25. Haq, S.; Hanke, F.; Dyer, M.S.; Persson, M.; Iavicoli, P.; Amabilino, D.B.; Raval, R. Clean Coupling of Unfunctionalized Porphyrins at Surfaces To Give Highly Oriented Organometallic Oligomers. *J. Am. Chem. Soc*. **2011**, *133*, 12031-12039.

26. Hanke, F.; Haq, S.; Raval R.; M.Persson. Heat to connect: Surface commensurability directs covalent one-dimensional self-assembly. *ACS Nano* **2011**, *5*, 9093-9103.

27. Ditze, S.; Stark, M.; Drost, M.; Buchner, F.; Steinruck, H.P.; Marbach, H. Activation Energy for the Self-Metalation Reaction of 2H-Tetraphenylporphyrin on Cu(111). *Angew. Chem. Int. Ed*. **2012**, *51*, 10898-10901.

28. Goldoni, A.; Pignedoli, C.A.; Di Santo, G.; Castellarin-Cudia, C.; Magnano, E.; Bondino, F . ; Verdini, A.; Passerone, D. Room Temperature Metalation of 2H-TPP Monolayer on Iron and Nickel Surfaces by Picking up Substrate Metal Atoms. *ACS Nano* **2012**, *6*, 10800-10807.

29. Davies, H.M.L.; Du Bois J.; Yu, J.-Q. C-H Functionalization in organic synthesis. *Chem. Soc. Rev.* **2011**, *40*, 1855-1856.

30. Siaj, M.; McBreen, P.H. Creating, varying, and growing single-site molecular contacts. *Science* **2005**, *309*, 588-590.

31. Carroll, R.L.; Gorman, C.B. The Genesis of Molecular Electronics. *Angew. Chem. Int. Ed.* **2002**, *41*, 4378–4400.

32. Dyer, M.S.; Robin, A.; Haq, S.; Raval, R.; Persson, M.; Klimes, J. Understanding the Interaction of the Porphyrin Macrocycle to Reactive Metal Substrates: Structure, Bonding, and Adatom Capture. *ACS Nano* **2011**, *5*, 1831-1838.

33. Pinardi, A.L.; Otero-Irurueta, G.; Palacio, I.; Martinez, J.I.; Sanchez-Sanchez, C.; Tello, M.; Rogero, C.; Cossaro, A.; Preobrajenski, A.; Gómez-Lor, B.; Jancarik, A.; Stará, I.G.; Starý, I.; Lopez, M.F.; Méndez, J.; Martin-Gago, J.A. Tailored Formation of N-Doped Nanoarchitectures by Diffusion-Controlled on-Surface (Cyclo)Dehydrogenation of Heteroaromatics. *ACS Nano* 2012, 7, 3676-3684.

34. Bieri, M.; Nguyen, M.T.; Groning, O.; Cai, J.M.; Treier, M.; Ait-Mansour, K.; Ruffieux, P. ; Pignedoli, C.A.; Passerone, D.; Kastler, M.; Mullen, K.; Fasel, R. Two-Dimensional Polymer Formation on Surfaces: Insight into the Roles of Precursor Mobility and Reactivity. *J. Am. Chem. Soc.* **2010**, *132*, 16669-16676.

35. Ditze, S.; Rockert, M.; Buchner, F.; Zillner, E.; Stark, M.; Steinruck, H.P.; Marbach, H. Towards the engineering of molecular nanostructures: local anchoring and

functionalization of porphyrins on model-templates *Nanotechnology* **2013**, *24*, Article Number: 115305.

36. Jones J.T.A.; Hasell, T.; Wu, X.F.; Bacsa, J.; Jelfs, K.E.; Schmidtmann, M.; Chong, S.Y.; Adams, D.J.; Trewin, A.; Schiffman, F.; Cora, F.; Slater, B.; Steiner, A.; Day, G.M.; Cooper, A.I. Modular and predictable assembly of porous organic molecular crystals. *Nature* **2011**, *474*, 367-371.

37. Zhu, Z.X.; Cardin, C.J.; Gan, Y.; Colquhoun, H.M. Sequence-selective assembly of tweezer molecules on linear templates enables frameshift-reading of sequence information. *Nature Chem*., **2010**, *2*, 653-660.

38. Deng, H.; Doonan, C.J.; Furukawa, H.; Ferreira, R.B.; Towne, J.; Knobler, C.B.; Wang, B.; Yaghi, O.M. Multiple functional groups of varying ratios in metal-organic frameworks. *Science*, **2010**, *327*, 846-850.

39. Lafferentz, L.; Ample, F.; Yu, H.; Hecht, S.; Joachim, C.; Grill, L. Conductance of a single conjugated polymer as a continuous function of its length. *Science*, **2009**, *323*, 1193-1197.

40. Barrett, S. D. Image SXM, (2012) http://www.ImageSXM.org.uk

41. Lin, V.S.Y.; Iovine, P.M.; DiMagno, S.G.; Therien, M.J. Dipyrryl and porphyrinic precursors to supramolecular conjugated (porphinato)metal arrays: Synthesis of dipyrrylmethane and (5,15-diphenylporphinato)zinc(II). In*organic Synthesis* **2002**, 33, 55-61

42. Kresse, G.; Furthmüller, Efficient iterative schemes for ab initio total-energy calculations using a plane-wave basis set. *Phys. Rev. B*, **1996**, 54, 11169.

43. Kresse, G.; Joubert, D. From ultrasoft pseudopotentials to the projector augmented-wave method. *Phys. Rev. B,* **1999**, 59, 1758.

44. Perdew, J.P.; Chevary, J.A.; Vosko, S.H.; Jackson, K.A; Pederson, M.R; Singh, D.J; Fiolhais, C. Atoms, molecules, solids, and surfaces- applications of the generalized gradient approximation for exchange and correlation. *Phys. Rev. B*. **1992**, 46, 6671.

45. Tersoff, J.; Hamann, D.R. Theory and application for the scanning tunneling microscope. *Phys. Rev. Lett*. **1983**, 50, 1998.

46. Lorente, N.; Persson, M. Theoretical aspects of tunneling-current-induced bond excitation and breaking at surfaces. *Faraday Discuss*. **2000**, 117, 277.

47. Perdew, J.P.; Burke, K.; Ernzerhof, M. Generalized Gradient Approximation Made Simple, *Phys. Rev. Lett*. 77 p3865 (**1996**)

48. Blum, V.; Gehrke, R.; Hanke, F.; Havu, P.; Havu, V.; Ren, X.; Reuter, K.; Scheffler, M. Ab initio molecular simulations with numeric atom-centered orbitals, *Comp. Phys. Comm*. **2009,** 180, 2175.

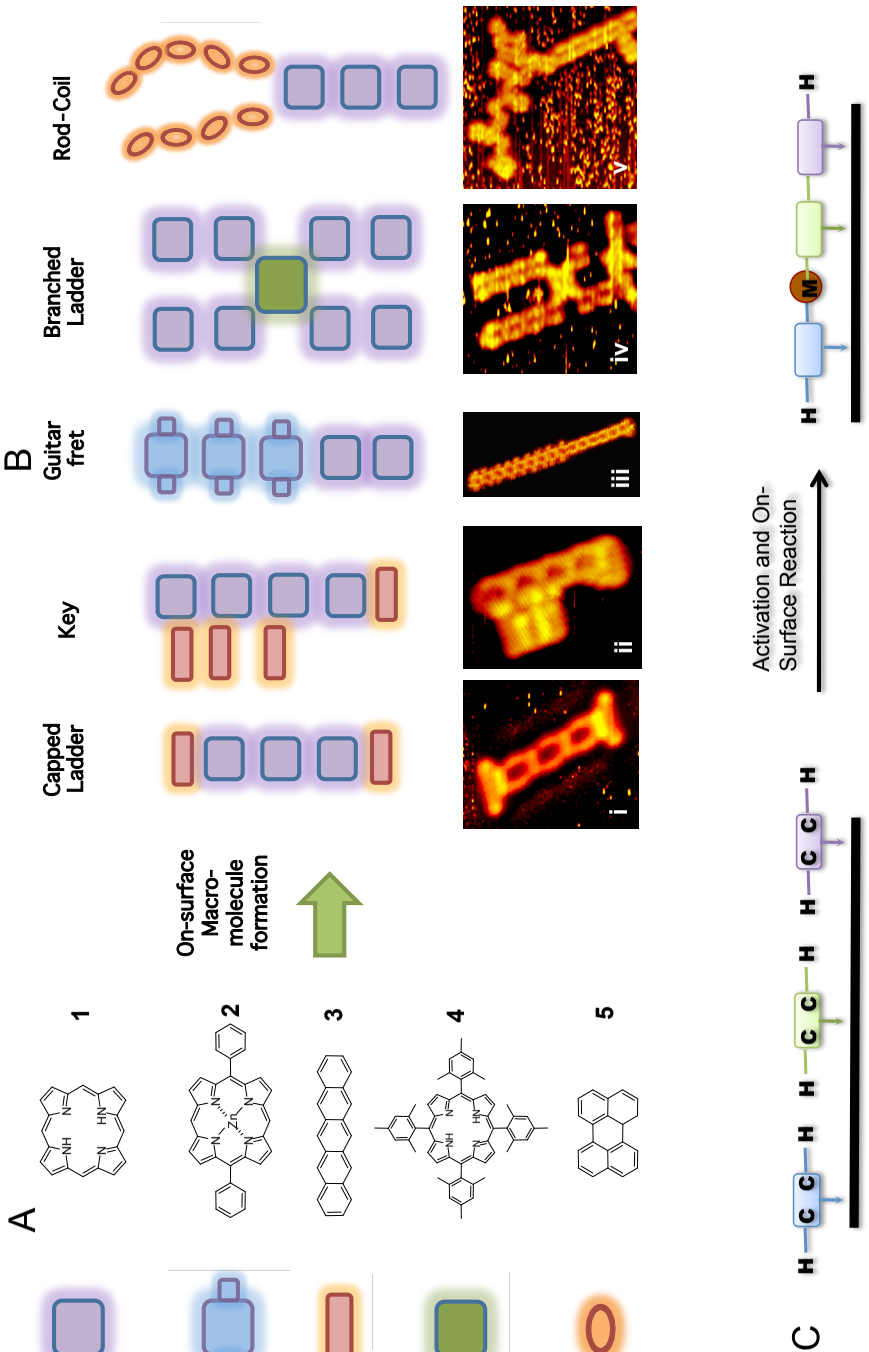

Figure 1. General overview of individual molecular building blocks and some of the hetero-organic macromolecules created using generic C-H bond activation at a Cu(110) surface.

A) Molecules used in this study: H_2-porphyrin (**1**), Zn(II)diphenylporphyrin (**2**), Pentacene (**3**), Tetramesitylporphyrin (**4**), and perylene (**5**), with their associated chemical structures and the simplified schematic representations, which are used to illustrate the range of complex macromolecules formed.
B) Examples of individual covalent heterostructures formed on the Cu(110) surface as imaged by STM: (i) **Capped Ladder**: 40 x 48 Å^2, I_t = 0.15 nA, V_t = - 1.40 V, (ii) **Key**: 45 x 65 Å^2, I_t = 0.2 nA, V_t = -1.96 V, (iii) **Guitar-fret**: 65 x 170 Å^2, I_t = 0.14 nA, V_t =-0.57V, (iv) **Branched Ladder**: 60 x 75 Å^2, I_t = 0.18 nA, V_t = - 1.28 V, (v) **Rod-Coil**: 100 x 100 Å^2, I_t = 0.11 nA, V_t = - 1.0 V.
C)Schematic showing general covalent coupling of organic components at a metal surface via C-H activation and formation of C-C and C-Metal-C organometallic bonds.

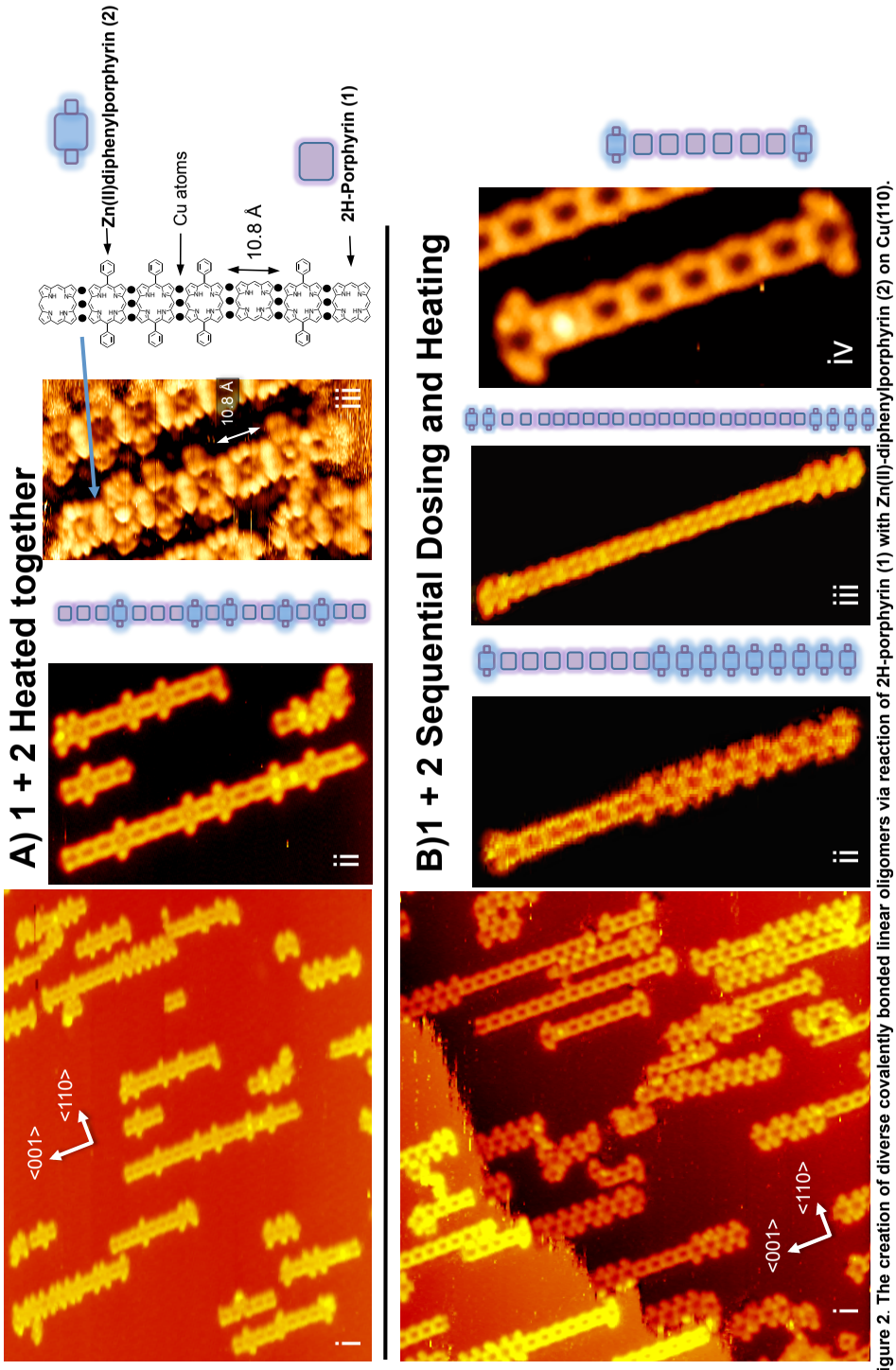

Figure 2. The creation of diverse covalently bonded linear oligomers via reaction of 2H-porphyrin (1) with Zn(II)-diphenylporphyrin (2) on Cu(110).

A)STM images obtained after both **1** and **2** are coadsorbed at 300 K and heated to 650K: (i) Large area image showing a range of products: 335 x 270 Å^2, I_t = 0.15nA, V_t = -1.27 V; (ii) Detail of a random co-polymer: 100 x 190 Å^2, I_t = 0.13 nA, V_t = - 1.68 V;(iii) high resolution STM image of a co-polymer chain showing the Cu atoms forming organometallic linkages: 35 x 70 Å^2, I_t = 0.17nA, V_t = -0.83 V.
B)STM images obtained following a sequential reaction protocol, in which (**1**) was dosed first, reacted at 650K to form chains, followed by adsorption of (**2**) and heating to 560K : (i) large area image, 300 x 300 Å^2, I_t = 0.07 nA, V_t = -1.1 V; (ii) '**Guitar-fret**' block copolymer structure, 65 x 170 Å^2, I_t = 0.14 nA, V_t =- 0.57 V, (iii) **Multiply capped** block polymer structure 90 x 265 Å^2, I_t = 0.15 nA, V_t = - 0.45 V, (iv) **Singly-capped** polymer structure, 40 x 85 Å^2, I_t = 0.06 nA, V_t = - 1.10 V

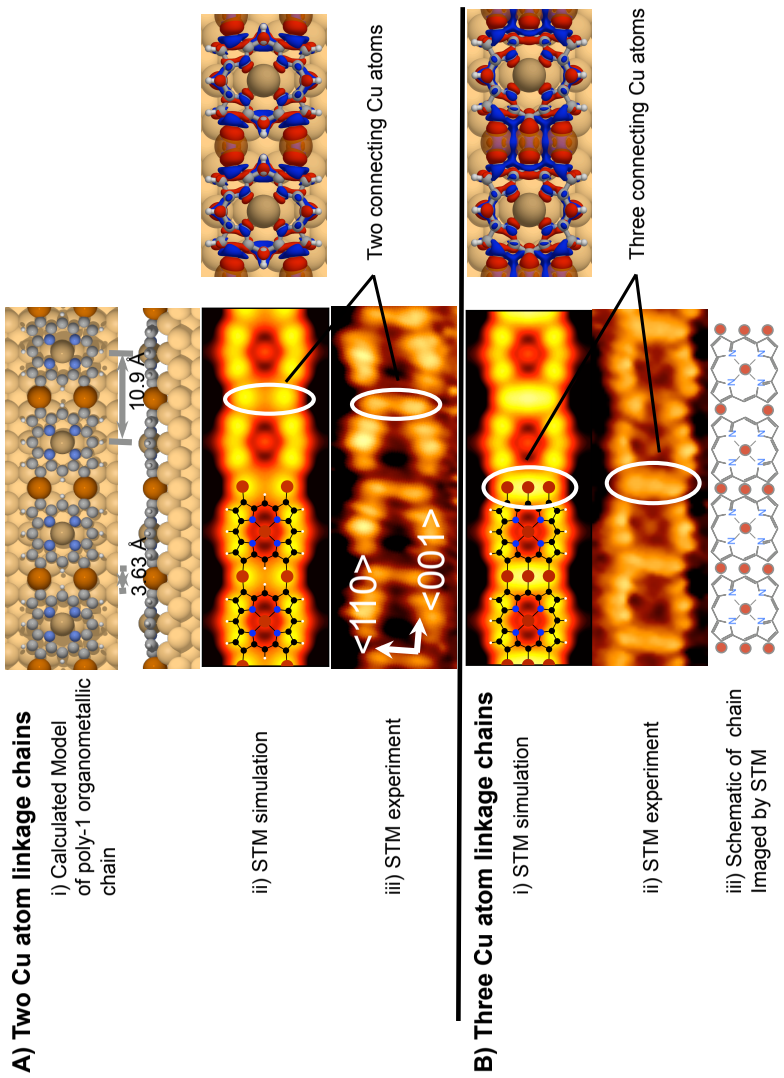

Figure 3: The nature of the Cu-porphyrin chain formed at the surface with 2 and 3 Cu adatom connection (adapted with permission, from ref 17).
A(i) Computed geometric structure of the Cu-porphyrin chain with a 2 Cu atom connection presenting top- and side-views showing the length scale and the bending of the porphyrin macrocycle toward the two connecting Cu atoms; A(ii) simulated STM images (4.36 nm x 1.54 nm, V_{tip} = -0.1 V) and A(iii) experimental STM image 4.45 nm x 1.4 nm (V_t= +0.4 V, I_t = 0.42 nA) showing submolecular detail of a 2 Cu atom coupled Cu-porphyrin nanowire.
B(i) Simulated STM images (4.36 nm x 1.54 nm, V_{tip} = -0.1 V) of a Cu-porphyrin nanowire with a 3 Cu atom connection. B(ii) experimental STM image 4.60 nm x 1.4 nm (V_t= -0.76 V, I_t = 0.19 nA) showing submolecular detail of a Cu-porphyrin nanowire with predominantly3 Cu atom connections and one 2 Cu atom connection. B(iii) shows a schematic representation identifying each connection.
The two images to the right of the STM data are calculated electron density differences for the 2 and 3 Cu atom connections respectively, indicating the bonding mechanisms for the C-Cu-C connection and the Cu-porphyrin-substrate interaction. The electron density difference is taken between the adsorbed system and the bare surface. Red and blue correspond to electron accumulation and depletion, respectively. Note that the connecting Cu atoms are partially transparent for clarity.

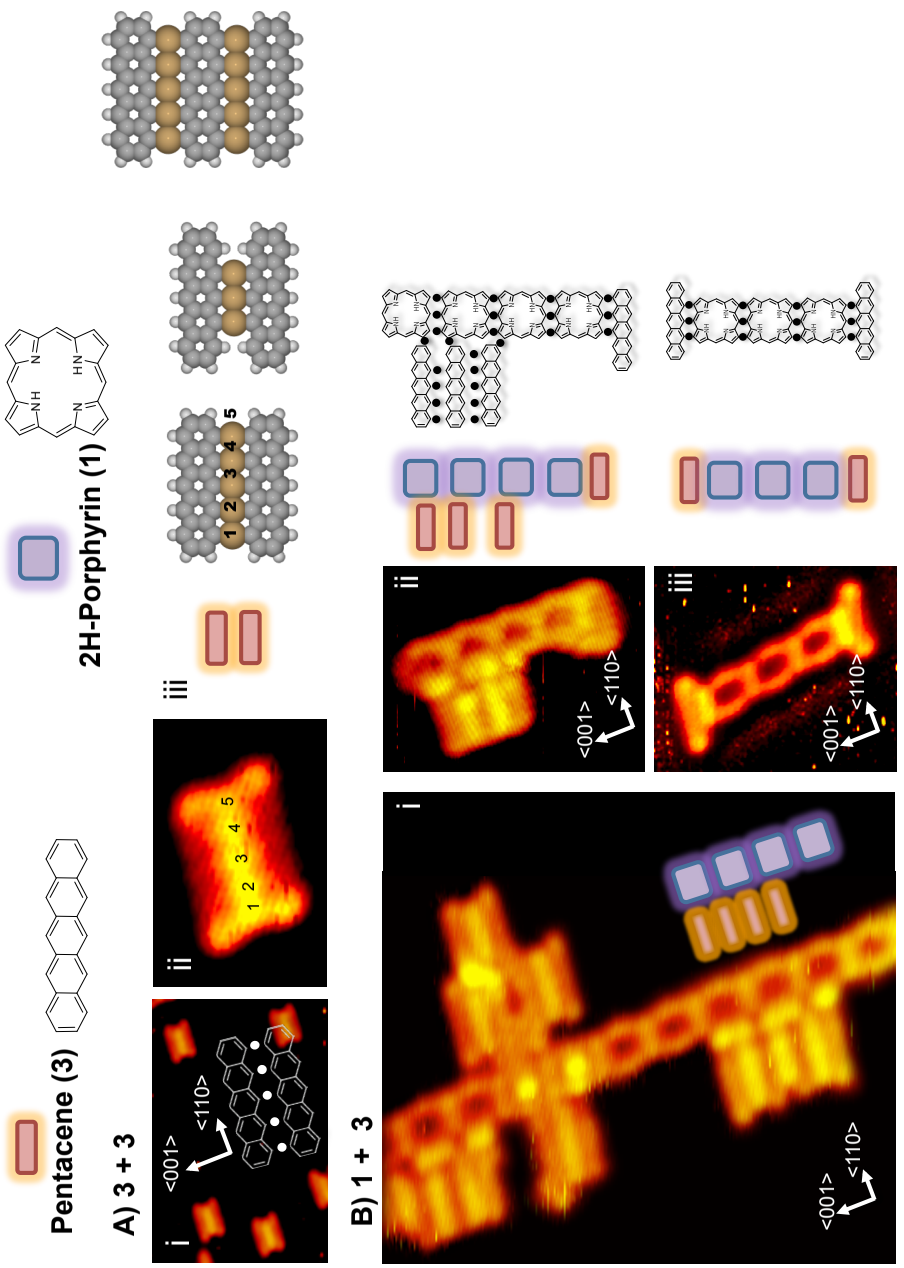

Figure 4: Covalently bonded structures formed by the reaction of pentacene (3) and 2H-porphyrin (1) at a Cu(110) surface.

A) STM images showing self-reaction of pentacene molecules to form covalently bonded organometallic dimer pairs after heating to 600 K: i) 110 x 65 Å^2, I_t = 0.11 nA, V_t = -1.16 V; ii) high resolution STM image of pentacene dimer with the 5 incorporated Cu atoms imaged bright and individually labeled 25 x 18 Å^2, I_t = 0.10 nA, V_t = -1.16V; (iii) hard sphere model of calculated structure with labeled Cu atoms..
B) STM images showing examples of heterostructures formed from the reaction of (**1**) and (**3**) by heating to 650 K: i) **Complex Key**: 90 x 85 Å^2, I_t = 0.15 nA, V_t =1.80 V, with schematic of lower portion; ii)**Simple Key**:45 x 65 Å^2, I_t = 0.2 nA, V_t = -1.96 V, with schematic on right; iii) **Pentacene Capped Porphyrin Chain**: 40 x 48 Å^2, I_t = 0.15 nA, V_t = -1.40 V, with schematic on right.

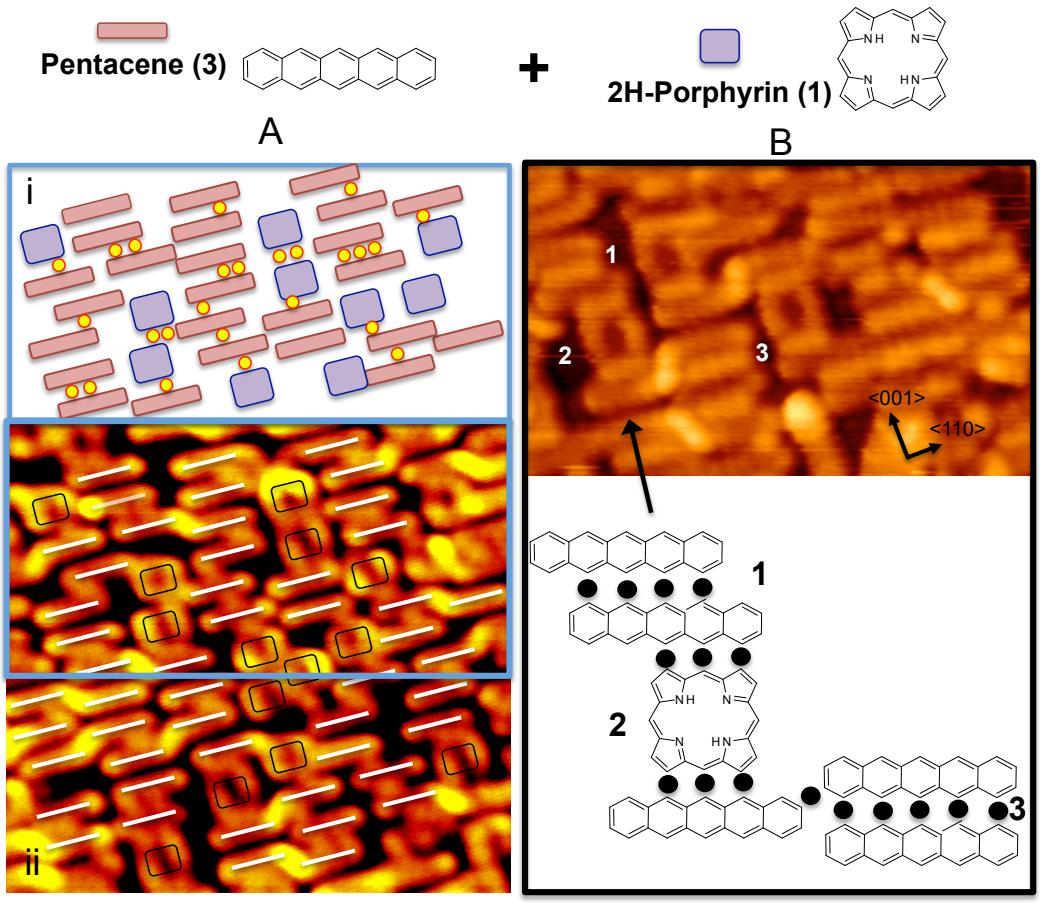

Figure 5. STM images obtained after porphyrin and pentacene are adsorbed at 300 K and heated to 650K. A(i) Schematic cartoon of top half of STM image below, depicting location of porphyrin, pentacene and Cu atoms. A(ii) STM image with some of the pentacene and porphyrin molecules highlighted with white lines and black squares, respectively: 100 x 120 Å^2, I_t = 0.08nA, V_t = -0.49 V. B) High resolution STM image obtained after porphyrin and pentacene are adsorbed at 300 K and heated to 650K. This shows the bonding, via imaged copper atoms, between the pentacene-pentacene, porphyrin-porphyrin and pentacene-porphyrin connections: 80 x 49 Å^2, I_t = 0.22 nA, V_t = - 0.71 V. Bottom part shows chemical schematic of the structure around the region labeled 1 - 3 in STM image below.

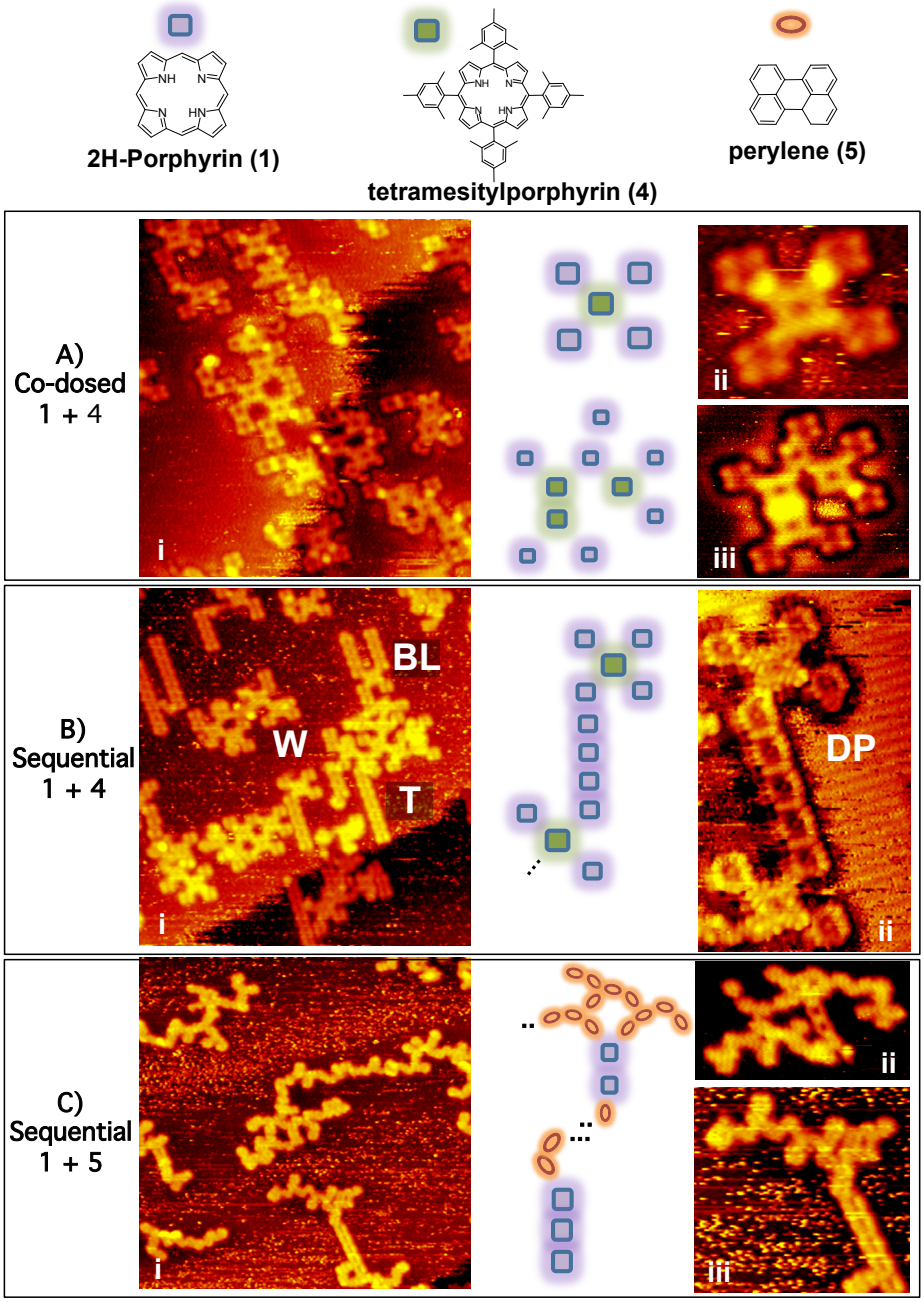

Figure 6. Mixed topology heterostructures formed on Cu(110) by combining different molecules that form rods (H_2-porphyrin 1), branches (trimesitylporphyrin 4) and coils (perylene 5).

A) Two-component branched structures formed by co-dosing H_2-porphyrin (**1**) and tetramesitylporphyrin (**4**) at 300 K and heated to 605K: (i) Large area STM image: 200 x 216 Å^2, I_t = 0.15nA, V_t = -1.24V; (ii) Small area STM showing a four-connected clover: 45 x 40 Å^2, I_t = 0.15nA, V_t = -1.24V; (iii) Small area STM showing a 2-component irregular branched motif: 65 x 60 Å^2, I_t = 0.15nA, V_t =-0.57V.

B) Creation of rod-branch macromolecules by initially reacting H_2-porphyrin (**1**) to 615 K to form chains and subsequently dosing tetramesitylporphyrin (**4**) and heating to 595K: (i) Large area STM image 300 x 324 Å^2, I_t = 0.18 nA, V_t = -1.28V; (ii) Small area STM showing a double propeller: 100 x 60 Å^2, I_t = 0.24 nA, V_t = - 0.78 V.

C) Creation of rod-coil macromolecules by co-dosing H_2-porphyrin (**1**) with perylene (**5**) together at room temperature and heating to 620K: (i) Large area STM image 300 x 300 Å^2, I_t = 0.11 nA, V_t = -1.0 V; Small area images of individual rod-coils (ii) 120 x 70 Å^2, I_t = 0.13nA, V_t =-1.44 V and (iii) 100 x 100 Å^2, I_t = 0.11 nA, V_t = -1.0 V.

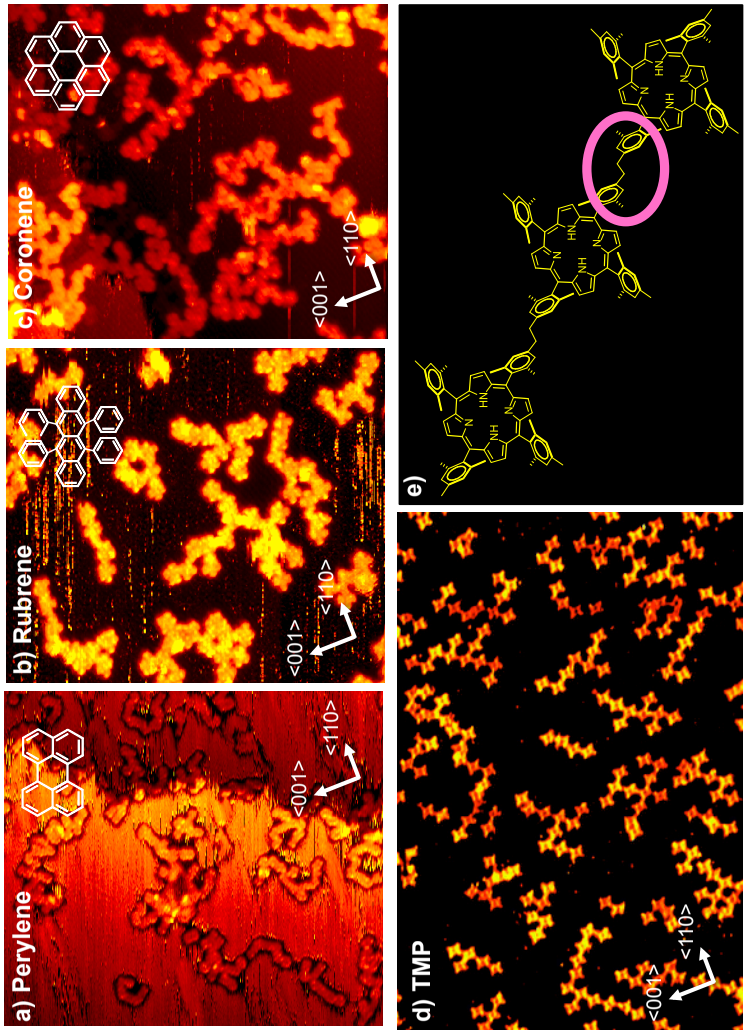

Figure 7. The creation of diverse C-C covalently bonded oligomers via reaction of arenes and porphyrins on Cu(110). a) STM image obtained after low coverage of perylene is adsorbed at 300 K and heated to 610K: 310 x 350 Å^2, I_t = 0.08nA, V_t = -0.63 V. Coil polymer structures are observed. b) STM image obtained after rubrene is adsorbed at 300 K and heated to 595K: 210 x 240 Å^2, I_t = 0.23nA, V_t = -1.49 V. c) STM image obtained after coronene is adsorbed at 300 K and heated to 605K: 310 x 350 Å^2, I_t = 0.19nA, V_t = -0.88 V. d) STM image after tetramesitylporphyrin (TMP) heated to 575 K on Cu(110: 550 x 380 Å^2, I_t = 0.50nA, V_t = -0.267 V. e) Chemical structure showing covalently bonding between TMP molecules.

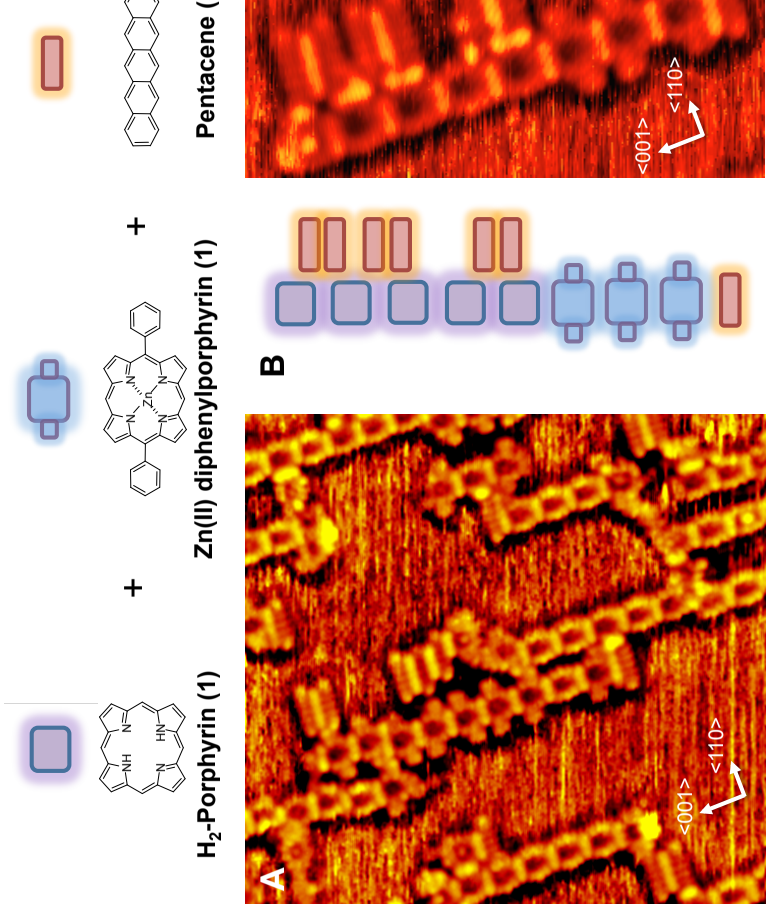

Figure 8. Three-component heterostructures formed by sequential reactions of H_2-porphrin (1), Zn(II)diphenylporphyrin (2) and pentacene(3).

A) Large area STM image (150 x 160 Å^2, I_t = 0.57nA, V_t = +0.34V) obtained following a sequential reaction protocol, in which (**1**) was dosed first and reacted at 650K to form chains, followed by adsorption of (**2**) and heating to 650K to make co-polymers, followed by adsorption of (5) and heating to 650K. Complex three-component macromolecular structures are observed, with bright protrusions between components revealing organometallic linkages via coupling Cu atoms.
B) Schematic and STM image of a 3-component key structure: 53 x 90 Å^2, I_t = 0.38 nA, V_t = +0.35 V.

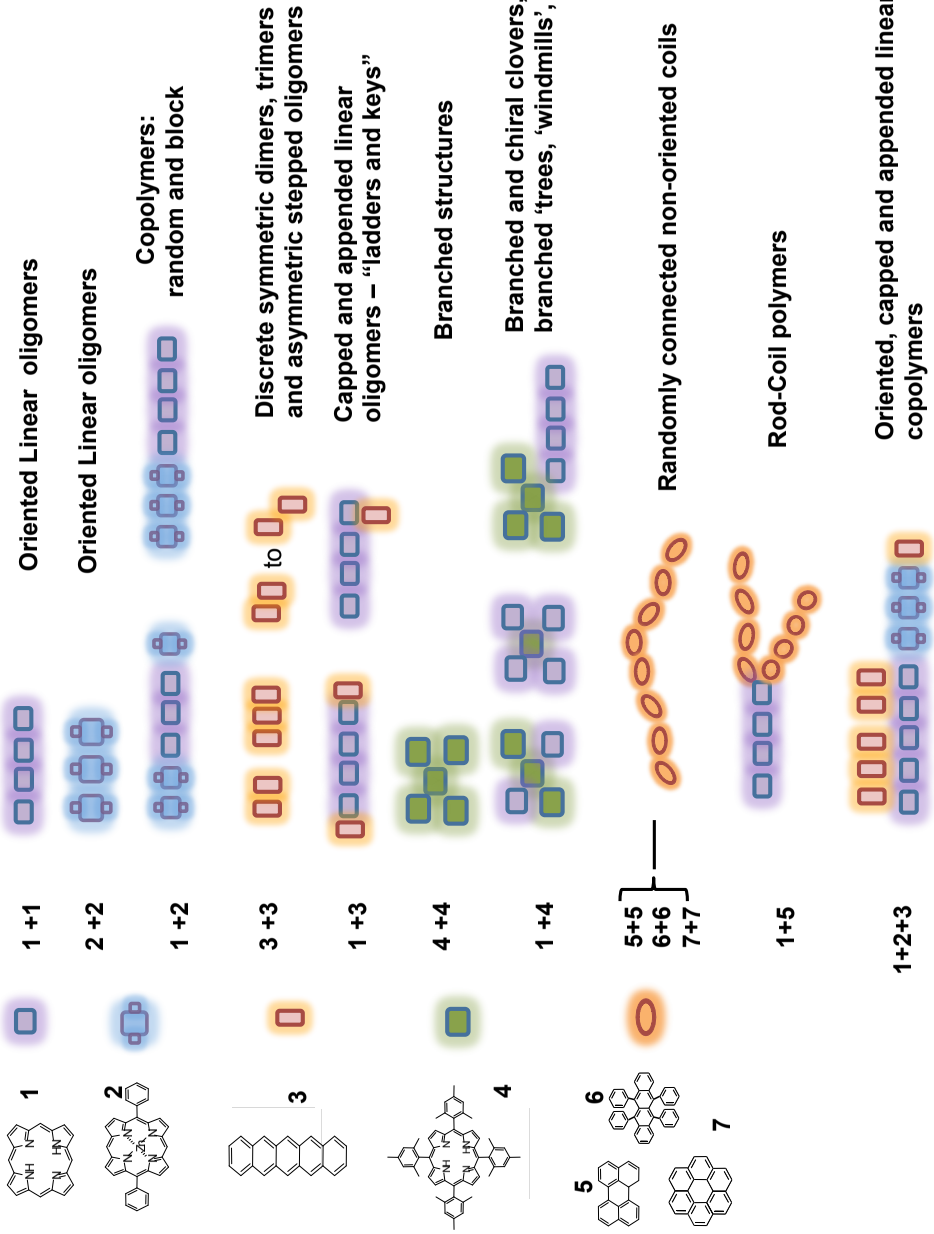

Figure 9. Summary of Molecules covalently linked on a Cu(110) surface in this study: 2H-porphyryin (1), Zn(II)diphenylporphyrin (2), Pentacene (3), Tetramesitylporphyrin (4), perylene (5), rubrene (6) and coronene (7) with their associated chemical structures and the simplified schematic representations, which are used to illustrate the diversity of complex macromolecules formed.

TEXT FOR TABLE OF CONTENTS

Title: Molecules picked, mixed and covalently linked at a surface via generic C-H bond activation to give macromolecular diversity.

Sam Haq, Felix Hanke, Mats Persson, David B. Amabilino and Rasmita Raval

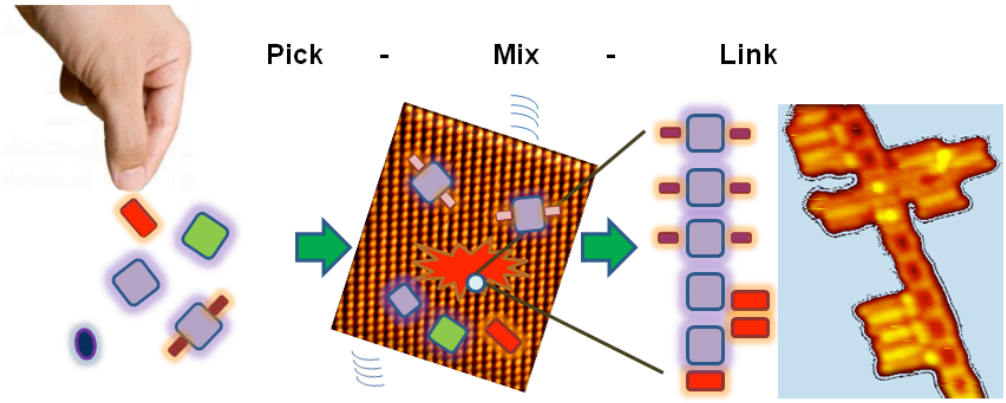

Different organic compounds are mixed at a surface and covalently coupled to provide complex and diverse macromolecules of differing topology and constitution.